Low-Q scaling, duality, and the EMC effect

J. Arrington,[1] R. Ent,[2] C. E. Keppel,[2,3] J. Mammei,[4,*] and I. Niculescu[5]
[1]*Argonne National Laboratory, Argonne, Illinois 60439, USA*
[2]*Thomas Jefferson National Accelerator Facility, Newport News, Virginia 23606, USA*
[3]*Hampton University, Hampton, Virginia 23668, USA*
[4]*Juniata College, Huntingdon, Pennsylvania 16652, USA*
[5]*James Madison University, Harrisonburg, Virginia 22807, USA*
(Received 3 October 2005; published 9 March 2006)

High energy lepton scattering has been the primary tool for mapping out the quark distributions of nucleons and nuclei. Data on the proton and deuteron have shown that there is a fundamental connection between the low and high energy regimes, referred to as quark-hadron duality. We present the results of similar studies to more carefully examine scaling, duality, and in particular the EMC effect in nuclei. We extract nuclear modifications to the structure function in the resonance region, and for the first time demonstrate that nuclear effects in the resonance region are identical to those measured in deep inelastic scattering. With the improved precision of the data at large x, we for the first time observe that the large-x crossover point appears to occur at lower x values in carbon than in iron or gold.

DOI: 10.1103/PhysRevC.73.035205 PACS number(s): 25.30.Fj, 13.60.Hb, 24.85.+p

I. INTRODUCTION

Extensive measurements of inclusive lepton-nucleus scattering have been performed in deep inelastic scattering (DIS) kinematics. In DIS kinematics, where both the four-momentum transfer, Q, and the energy transfer, ν, are sufficiently large, the extracted structure function exhibits scaling, i.e., is independent of Q^2 except for the well understood logarithmic QCD scaling violations. In this region, the structure function is interpreted as an incoherent sum of quark distribution functions, describing the motion of the quarks within the target.

Such measurements have unambiguously shown that the nuclear structure functions deviate from the proton and neutron structure functions. Such modifications, termed the EMC effect after the first experiment to observe them [1], demonstrate that the nuclear quark distribution function is not just the sum of the proton and neutron quark distributions. Within two years of the first observation, hundreds of papers were published on the topic. After 20 years of experimental and theoretical investigation, the effect still remains a mystery. For detailed reviews of the data and models of the EMC effect, see Refs. [2,3]

Existing measurements of the EMC effect indicate little Q^2 dependence, and an A dependence in the magnitude, but not the overall form, of the structure function modification in nuclei. The nature of the modifications in nuclei depends primarily on Bjorken-x, $x = Q^2/2M\nu$, where in the parton model x is interpreted as the momentum fraction of the struck quark, and the nuclear effects are divided into four distinct regions. In the shadowing region, $x < 0.1$, the structure function is decreased in nuclei relative to the expectation for free nucleons. In the antishadowing region, $0.1 < x < 0.3$, the structure function shows a small nuclear enhancement. For $0.3 < x < 0.7$, referred to as the EMC effect region, the nuclear structure function shows significant depletion. Finally, there is a dramatic enhancement as x increases further, resulting from the increased Fermi motion of the nucleons in heavier nuclei.

Explanations of the EMC effect are hampered by the lack of a single description that can account for the nuclear dependence of the quark distributions in all of these kinematic regimes. Here, we will limit ourselves to $x > 0.3$, the region where valence quarks dominate. Even in this limited region, there is not a single explanation that can completely account for the observed nuclear structure function modifications. If the nuclear structure function in this region is expressed as a convolution of proton and neutron structure functions, there are two alternative approaches used to describe the observed medium effect: (1) incorporating nuclear physics effects that modify the energy-momentum behavior of the bound proton with respect to the free proton, or (2) incorporating changes to the internal structure of the bound proton. It has been argued, most recently in Ref. [4], that the binding of nucleons alone cannot explain the EMC effect. In addition, several attempts to explain the EMC effect in terms of explicit mesonic components appear to be ruled out due to limits set by Drell-Yan measurements [5]. Hence, the EMC effect may be best described in terms of modifications to the internal structure of the nucleon when in the nuclear environment.

We note that while the EMC effect has been mapped out over a large range of x, Q^2, and A, information is still rather limited in some regions. There are limited data on light nuclei ($A < 9$), and almost no data in the DIS regime at extremely large x, where the quark distributions in nuclei are enhanced due to the effects of binding and Fermi motion. Since binding and Fermi motion impact the EMC ratios for all x values, it is important to be able to constrain these effects in a region where other, more exotic, explanations are not expected to contribute. It should be possible to learn more about the EMC effect at large x by taking advantage of the extended scaling

*Present address: Virginia Tech, Blacksburg, Virginia 24061, USA.

of structure functions in nuclei [6,7]. In this paper, we attempt to quantify the deviations from perturbative scaling at large x, with the goal of improving measurements of the structure functions and the EMC ratios at large x.

II. SCALING OF THE NUCLEAR STRUCTURE FUNCTION

Inspired by a recent series of electron scattering experiments in Hall C at Jefferson Lab, we revisit the issues of scaling in nuclear structure functions and the EMC effect. The Hall C data are at lower invariant mass W, $W^2 = M_p^2 + 2M_p\nu(1-x)$, and therefore higher x, than data thus far used to investigate the EMC effect. Most notably, these new data are in the resonance region, $W^2 < 4$ GeV^2. In the DIS region, $W^2 > 4$ GeV^2, the Q^2 dependence of the structure functions is predicted by perturbative QCD (pQCD), while additional scaling violations, target mass corrections and higher twist effects, occur at lower Q^2 and W^2 values. Thus, data in the resonance region would not naively be expected to manifest the same EMC effect as data in the deep inelastic scaling regime. The effect of the nuclear medium on resonance excitations seems non-trivial, and may involve much more than just the modification of quark distributions observed in DIS scattering from nuclei.

However, while resonance production may show different effects from the nuclear environment, there are also indications that there is a deeper connection between inclusive scattering in the resonance region and in the DIS limit. This connection has been a subject of interest for nearly three decades since quark-hadron duality ideas, which successfully described hadron-hadron scattering, were first extended to electroproduction. In the latter, Bloom and Gilman [8] showed that it was possible to equate the proton resonance region structure function $F_2(\nu, Q^2)$ at low Q^2 to the DIS structure function $F_2(x)$ in the high-Q^2 scaling regime, where F_2 is simply the incoherent sum of the quark distribution functions. For electron-proton scattering, the resonance structure functions have been demonstrated to be equivalent on average to the DIS scaling strength for all of the spin averaged structure functions (F_1, F_2, F_L) [9,10], and for some spin dependent ones (A_1) [11] (for a review of duality measurements, see Ref. [12]).

The goal of this paper is to quantify quark-hadron duality in nuclear structure functions and to determine to what extent this can be utilized to access poorly understood kinematic regimes. While the measurements of duality from hydrogen indicate that the resonance structure function are on average equivalent to the DIS structure functions, it has been observed that in nuclei, this averaging is performed by the Fermi motion of the nucleons, and so the resonance region structure functions yield the DIS limit without any additional averaging [6,7].

Figure 1 shows the structure functions for hydrogen [9], deuterium [16], and iron [7], compared to structure functions from MRST [13] and NMC [14] parametrizations. Each set of symbols represents data in a different Q^2 range, with the highest Q^2 curves covering the highest ξ values. Note that the data are plotted as a function of the Nachtmann variable, $\xi = 2x/(1+\sqrt{1+4M^2x^2/Q^2})$, rather than x. In the limit

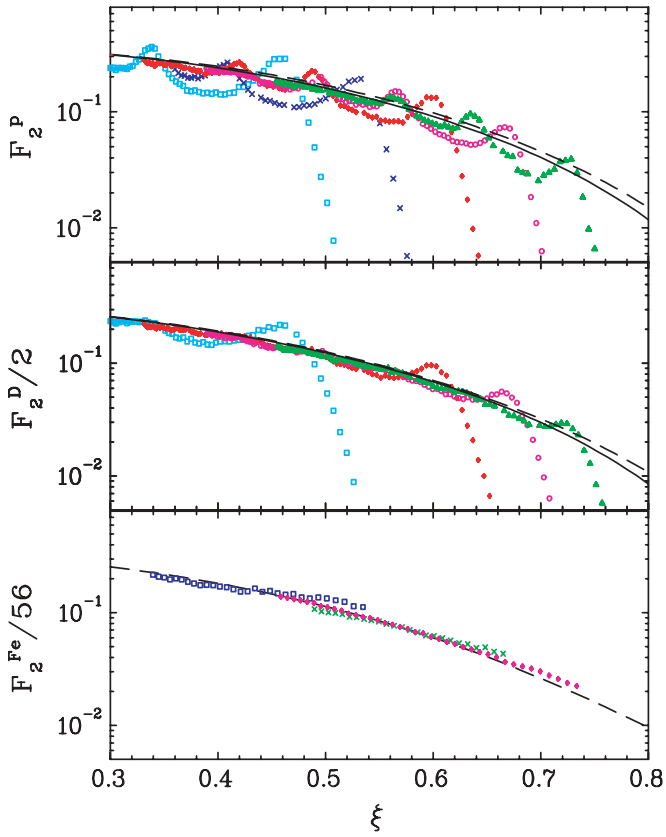

FIG. 1. (Color online) The F_2 structure function per nucleon vs ξ for hydrogen (top), deuterium (middle), and iron (bottom). For the hydrogen and deuterium data ($0.8 < Q^2 < 3.3$ GeV^2), the elastic (quasielastic) data have been removed. For the iron data ($Q^2 < 5.0$ GeV^2), a cut of $W^2 > 1.2$ GeV^2 is applied to remove the quasielastic peak. The curves are the MRST [13] (solid) and NMC [14] (dashed) parametrizations of the structure functions at $Q^2 = 4$ GeV^2, with a parametrization of the EMC effect [15] applied to produce the curve for iron.

of large Q^2, $\xi \to x$, and so ξ can also be used to represent the quark momentum in the Bjorken limit. At finite Q^2, the use of ξ reduces scaling violations related to target mass corrections [17]. The difference between ξ and x is often ignored in high energy scattering or at low x, but cannot be ignored at large x or low Q^2. The goal is to examine ξ-scaling to look for any significant scaling violations beyond the known effects of perturbative evolution and target mass corrections. Examining the scaling in terms of ξ instead of x is only an approximate way of applying target mass corrections, but it is a reasonable approximation to a more exact correction [17] in the case of the proton, and the appropriate prescription for target mass corrections in nuclei is not as well defined.

The transition from scaling on average in the proton to true scaling for nuclei is clearly visible. There is significant resonance structure visible in hydrogen, but on average the structure function reproduces the scaling curve to better than 2% globally and 5% locally around each resonance for $Q^2 > 1$ GeV^2 [9]. For deuterium, Fermi motion and other medium effects broaden the resonances to the point where only the Δ resonance has a clear peak, and the data at higher W^2 values,

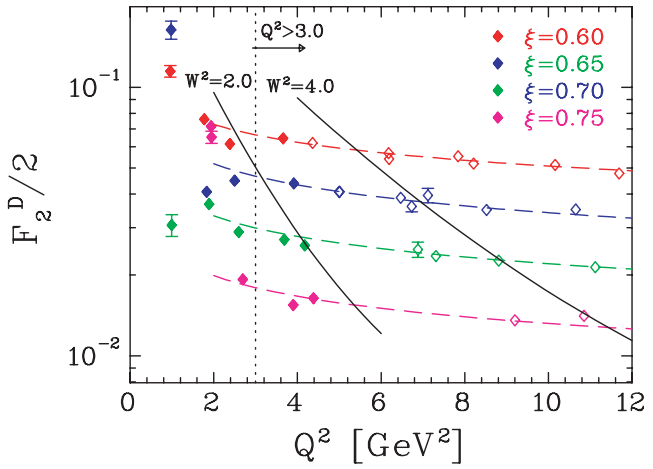

FIG. 2. (Color online) F_2 structure function per nucleon vs Q^2 for deuterium at fixed values of ξ. Dashed lines show a logarithmic Q^2 dependence, with the value of $d \ln F_2/d \ln Q^2$ determined at each ξ value from SLAC data at high Q^2 (up to 20 GeV^2). The solid lines denote $W^2 = 2.0$ and 4.0 GeV^2. The combined statistical and systematic uncertainties are shown. The hollow symbols are data from SLAC [18], while the solid symbols are from Jefferson Lab [7].

while still in the resonance region, is indistinguishable from the scaling curve except at the lowest Q^2 values. For the iron data, taken at somewhat higher Q^2 values, even the Δ is no longer prominent, and deviations from pQCD predictions are small, and limited to the tail of the quasielastic peak.

We can study the quality of scaling in the resonance region more directly by examining the Q^2 dependence of the structure function at fixed ξ. Figure 2 shows the Q^2 dependence of the structure function for several values of ξ. Above $W^2 = 4$ GeV^2, the data are in the DIS region and the Q^2 dependence is consistent with the logarithmic Q^2 dependence from QCD evolution (dashed lines). Even at lower W^2, where the data are in the resonance region, scaling violations are small. Above $Q^2 = 3$ GeV^2, the data deviate from the logarithmic Q^2 dependence by $\lesssim$10%, even down to $W^2 = 2$ GeV^2. Data on heavier nuclei show a similar extended scaling in the resonance region, as seen in Fig. 3 of Ref. [7], although the largest scaling violations (in the vicinity of the quasielastic peak) are smaller, due to the increased Fermi smearing.

Analyses of duality for the proton [19] and for nuclei [20,21] show that the moments of the structure function, $M_n = \int x^{n-2} F_2(x, Q^2) dx$ is the nth moment, follow perturbative QCD evolution down to $Q^2 \approx 2$ GeV^2 for the proton and to even lower values, $Q^2 \lesssim 1$ GeV^2, for nuclei. The fact that the moments follow the perturbative behavior is consistent with the observation that the structure function in Figs. 1 and 2 are, on average, in agreement with the perturbative structure function.

The data indicate relatively small deviations from pQCD for $Q^2 > 3$ GeV^2 at all values of ξ measured. These deviations decrease as Q^2 increases, making the nuclear structure functions at large ξ consistent with the perturbative dependence even at values of W^2 well below the typically DIS limit. The limited kinematics coverage of the existing data make it difficult to precisely map out deviations from perturbative evolution. There is a large gap in Q^2 between the JLab data shown here and the SLAC measurements at large Q^2. The situation will be improved by the recently completed measurements from JLab experiments E03-103 and E00-116 [22,23], which will provide more complete ξ coverage over a wide range in Q^2. In the meantime, Fig. 2 indicates that for $Q^2 \gtrsim$ 3–4 GeV^2, one can relax the usual DIS requirement that $W^2 > 4$ GeV^2, and the structure functions measured in the resonance region will still provide a good approximation to the DIS structure functions.

Even with the uncertainties arising from possible higher twist contributions, data at large ξ can significantly improve our knowledge of the high-ξ nuclear structure functions. There is very little DIS data for $\xi \gtrsim 0.8$, and no existing facility has the combination of energy and luminosity necessary to make precise measurements of in this regime, which requires $Q^2 > 15(36)$ GeV^2 for $\xi > 0.8(0.9)$. If we can set reasonable limits on scaling violations at fixed ξ due to possible higher twist contributions, we can provide useful data in this region where the few existing measurements of the EMC effect have 10–20% uncertainties.

III. STRUCTURE FUNCTION RATIOS

Because of the difficulty in making precise measurements in the DIS region at large ξ, existing measurements of the EMC effect in this region are very poor. At large ξ, the EMC effect should be dominated by binding effects and Fermi motion. Constraining these effects will allow a better separation of these "conventional" nuclear effects, which are important at all ξ values, from more exotic effects that have been used to explain the EMC effect at lower ξ.

We can examine the EMC effect in the resonance region using recent measurements [7] of inclusive scattering from deuterium, carbon, iron, and gold. For these data, we take the cross section ratio of iron to deuterium *in the resonance region* for the highest Q^2 measured ($Q^2 \sim 4$ GeV^2), requiring $W^2 >$ 1.2 GeV^2 to exclude the region very close to the quasielastic peak.

There are small differences between the analyses of the SLAC and JLab data which had to be addressed to make a precise comparison. First, the SLAC and BCDMS ratios were extracted as a function of x rather than ξ. Because the conversion from x to ξ depends on Q^2, we can only compare ratios extracted at fixed Q^2 values. Thus, for E139 we use the "coarse-binned" ratios, evaluated at fixed Q^2, rather than "fine" x binning, which were averaged over the full Q^2 range of the experiment. Coulomb corrections were applied in the analysis of the JLab data [24], but not the SLAC data. The SLAC data shown here include Coulomb corrections, determined by applying an offset to the incoming and outgoing electron energy at the reaction vertex [24], due to the Coulomb field of the nucleus. The correction factor is <0.5% for carbon, and (1.5–2.5)% for gold. The JLab and SLAC ratios are corrected for neutron excess, assuming $\sigma_n/\sigma_p = (1 - 0.8\xi)$.

Figure 3 shows the cross section ratio of heavy nuclei to deuterium for the previous SLAC E139 [15], E87 [25], and

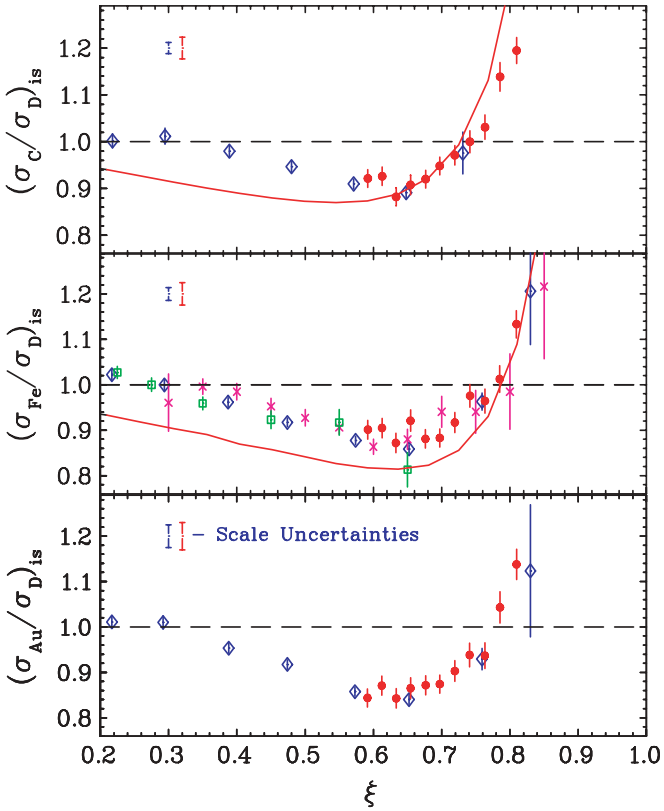

FIG. 3. (Color online) Ratio of nuclear to deuterium cross section per nucleon, corrected for neutron excess. The solid circles are Jefferson lab data taken in the resonance region ($1.2 < W^2 < 3.0$ GeV^2, $Q^2 \approx 4$ GeV^2). The hollow diamonds are SLAC E139 data, the crosses are the SLAC E87 data, and the hollow squares are BCDMS data, all in the DIS region. The scale uncertainties for the SLAC (left) and JLab (right) data are shown in the figure. The curves show an updated version [27] of the calculations from Ref. [28].

BCDMS [26] DIS measurements, and for the JLab E89–008 [7,24] data in the resonance region. The size and ξ dependence of nuclear modifications in the JLab data agrees with the higher Q^2, W^2 data for all targets. Table I shows the ratios extracted from the JLab data.

The agreement of the resonance region data with the DIS measurement of the EMC effect, which directly measures the modification of quark distributions in nuclei, is quite striking. There is no *a priori* reason to expect that the nuclear effects in resonance production would be similar to the effects in scattering from quarks. However, it can be viewed as a natural consequence of the quantitative success of quark-hadron duality [9,12]. As seen in Fig. 1, the structure functions for nuclei show little deviation from pQCD, except in the region of the quasielastic peak (and Δ resonance at low Q^2). As Q^2 increases, the deviations from pQCD decrease as quasielastic scattering contributes a smaller fraction of the cross section. In retrospect, given the lack of significant higher twist contributions, combined with the fact that any A-independent scaling violations will cancel in the ratio, it is perhaps not surprising that the resonance EMC ratios are in agreement with the DIS measurements.

TABLE I. Isoscalar EMC ratios for carbon, iron, and gold in the resonance region extracted from the data of Ref. [7]. W^2 is calculated using the nucleon mass, rather than the nuclear mass.

ξ	W^2 GeV^2	$(\sigma_C/\sigma_D)_{is}$	$(\sigma_{Fe}/\sigma_D)_{is}$	$(\sigma_{Au}/\sigma_D)_{is}$
0.592	2.86	0.921 ± 0.012	0.901 ± 0.013	0.844 ± 0.013
0.613	2.70	0.926 ± 0.013	0.905 ± 0.014	0.871 ± 0.015
0.633	2.55	0.882 ± 0.013	0.872 ± 0.015	0.843 ± 0.016
0.654	2.39	0.908 ± 0.014	0.921 ± 0.017	0.865 ± 0.017
0.676	2.22	0.920 ± 0.012	0.881 ± 0.012	0.872 ± 0.014
0.697	2.07	0.948 ± 0.011	0.883 ± 0.010	0.874 ± 0.013
0.719	1.91	0.971 ± 0.013	0.917 ± 0.012	0.903 ± 0.016
0.741	1.75	1.000 ± 0.016	0.976 ± 0.015	0.938 ± 0.020
0.763	1.59	1.031 ± 0.019	0.964 ± 0.017	0.937 ± 0.023
0.786	1.43	1.139 ± 0.022	1.013 ± 0.020	1.043 ± 0.028
0.810	1.26	1.195 ± 0.014	1.133 ± 0.015	1.138 ± 0.024

While it is difficult to precisely quantify the higher twist contributions with the present data, we can estimate their effect by looking at low W^2 and Q^2, where the higher twist contributions are much larger. At $Q^2 \approx 2$ GeV^2 and $W^2 \approx M_\Delta^2$, the scaling violations (beyond target mass corrections) for deuterium are as large as 50%, as seen in Fig. 1. However, if one takes the iron and deuterium data from Ref. [7], *averages* the structure function over the Δ region and then forms the EMC ratio, the result differs from the ratio in the DIS region by less than 10%. The decrease in the effect of higher twist contributions is a combination of the fact that the contribution are reduced when averaged over an adequate region in W^2 [9,12], and cancellation between the higher twist contributions in deuterium and iron. The same procedure yields 2–3% deviations from the EMC ratio if one looks in the region of the S_{11} or P_{15} resonances, where the scaling violations in the individual structure functions are smaller to begin with.

For the ratios in Fig. 3, we expect even smaller higher twist effects because the data is nearly a factor of two higher in Q^2 and is above the Δ except for the very highest ξ points. At higher Q^2, the higher twist contributions in the individual structure functions become smaller, while averaging over the resonance region becomes less important as the resonances become less prominent. Thus, we expect that higher twist contributions for these data will be smaller than the the 2–3% effect (<10% near the Δ) observed on the EMC ratio at $Q^2 \approx 2$ GeV^2. If so, the higher twist corrections will be small or negligible compared to the large statistical uncertainty in previous measurements, and this data can be used to improve our knowledge of the EMC effect at large ξ.

IV. THE EMC EFFECT AT LARGE $x(\xi)$

A careful examination of the crossover point at large ξ, where the ratio $(\sigma_A/\sigma_D)_{is}$ becomes larger than unity, reveals that this appears to occurs at larger ξ for heavy nuclei than for light nuclei. This behavior is consistent with the SLAC data, but the large-ξ coverage of the previous measurements was insufficient to make a clear statement about the crossover point. This observation contradicts the argument that the dramatic enhancement at large ξ is simply due to

increased Fermi motion in heavy nuclei relative to deuterium. In this simple picture, the slight increase in Fermi motion as one goes to heavier nuclei would lead to an earlier onset of this enhancement. While the Coulomb corrections and neutron excess corrections do affect the A dependence, the uncertainties on these corrections are not large enough to explain the observed differences between carbon and heavier nuclei.

Within the convolution formula of proton and neutron structure functions, this crossover comes about due to counteracting contributions at large ξ of the average nucleon binding energy and average kinetic energy [29], and is hardly expected to change for $A > 10$. More detailed calculations have been done to determine the effect of binding and Fermi motion, but except for calculations of ^{3,4}He, most of these calculations were performed for a Fermi gas model or for infinite nuclear matter, with the density varied to approximate the finite nuclei. These calculations do not show any significant change in the ξ dependence for heavy ($A > 10$) nuclei. Because of the lack of precise data at large x, especially with respect to the A-dependence, realistic models of the nuclear structure were generally not considered to be necessary.

The effect we observe was predicted in a calculation by Gross and Liuti [28] using a manifestly covariant form of the convolution formula. The most significant improvement with respect to traditional binding models is in the active role played by the transverse degrees of freedom; namely, the transverse momenta of both the struck quark and proton, which generates terms beyond the light cone convolution formula. This yields a different interplay between the Fermi motion and binding (off-shell) effects than other binding models, providing a mechanism that generates an additional nuclear dependence to the high-ξ crossover point. Their calculation predicts a shift in the high-ξ crossover point between carbon and iron, somewhat larger than is observed in the data. An updated version [27] of this calculation is shown for carbon and iron in Fig. 3. Additional details of the calculation can be found in Ref. [30], which differs from the version shown here only in the low-ξ region. Another calculation including A-dependent nuclear spectral functions [31] also gave an A-dependent crossover point at large ξ. However, this calculation had the crossover point moving to *lower* ξ values for heavier nuclei.

Other models of the EMC effect have looked at physics beyond Fermi motion and binding. As with the binding models, they generally did not attempt to reproduce the detailed A-dependence, and instead evaluated the EMC effect for nuclear matter as a function of density. Most of these models were designed to describe the excess strength at lower ξ, and in general they do not significantly impact the structure function at large ξ. Thus, the addition of improved EMC ratio measurements at large ξ and the observation of an A dependence to the high-ξ behavior is most important in constraining the portion of the EMC effect that is related to binding. One can see from the calculations shown in Fig. 3 that the effects of binding and Fermi motion are important over the entire ξ region, and not just at the largest ξ values. These conventional nuclear effects must be well constrained to establish a reliable baseline before one can isolate any additional nuclear modification at lower x values that might require a more exotic explanation. Improved data at large ξ and for a variety of nuclei should allow for tests of the prescriptions chosen for binding and Fermi motion, and thus provide a more reliable baseline for models of the EMC effect.

The modified x dependence in carbon also appears to contradict the conclusions of a recent effective field theory calculation of the EMC effect that predicts factorization of the A and x dependence, and thus the universality of the x dependence [32]. The change in the high-x crossover in the present data is small, but a recent measurement of the EMC effect for ^{3}He and ^{4}He [22] will provide a more sensitive test of the universality of the x dependence.

V. CONCLUSIONS

This analysis provides not only an increase in the ξ range of the measurements of nuclear structure functions, but also the first observation of an A dependence of the high-ξ behavior of the EMC effect. Measurements utilizing higher energy beams will extend measurements of the EMC effect to even larger ξ values. Based on the results shown here, the uncertainties on extracting the EMC effect at large ξ due to higher twist contributions will be small, if not negligible, compared to the uncertainties of existing data. A recent measurement at Jefferson Lab [22] will extend measurements of the EMC effect to larger ξ values and to light nuclei, where few-body calculations can be performed with significantly smaller uncertainties coming from uncertainties in the nuclear structure. The calculations of Ref. [28] predict that the high-ξ crossover point in carbon occurs at lower ξ than in heavier nuclei, as was observed in the data. However, they predict a crossover at much *larger* ξ for ^{4}He. Similarly, Ref. [33] also predicts a different high-ξ behavior in ^{4}He than in heavy nuclei, and in addition predicts a significant difference between ^{3}He and ^{4}He.

Similar investigations of duality and scaling in polarized and separated structure functions are underway [34–36]. If duality in these processes is quantitatively as successful as in this case, this will have a similar impact on our ability to measure high-ξ polarized structure functions.

In conclusion, we present the first extraction of the nuclear dependence of the inclusive structure function in the resonance region. The data are in agreement with previous measurements of the nuclear dependence of the quark distributions in DIS scattering measurements of the EMC effect. This surprising result can be understood in terms of quark-hadron duality, where the structure function in the resonance regime is shown to have the same perturbative QCD behavior as in the DIS regime. These data expand the ξ and Q^2 range of such measurements, and provide the first new measurement of the EMC effect for a decade. They also indicate the possibility for dramatic improvements in both the ξ and A range in future measurements, using the higher beam energies currently available at Jefferson Lab.

ACKNOWLEDGMENTS

We thank Simonetta Liuti for providing updated calculations, and Dave Gaskell for useful discussions. This work was supported in part by DOE Grant Nos. W-31-109-ENG-38 and DE-FG02-95ER40901, and NSF Grant 0099540.

[1] J. Aubert *et al*., Phys. Lett. **B123**, 275 (1983).
[2] M. Arneodo, Phys. Rep. **240**, 301 (1994).
[3] D. F. Geesaman, K. Saito, and A. W. Thomas, Annu. Rev. Nucl. Sci. **45**, 337 (1995).
[4] J. R. Smith and G. A. Miller, Phys. Rev. C **65**, 055206 (2002).
[5] D. M. Alde *et al*., Phys. Rev. Lett. **64**, 2479 (1990).
[6] B. W. Filippone *et al*., Phys. Rev. C **45**, 1582 (1992).
[7] J. Arrington *et al*., Phys. Rev. C **64**, 014602 (2001).
[8] E. Bloom and F. Gilman, Phys. Rev. D **4**, 2901 (1971).
[9] I. Niculescu *et al*., Phys. Rev. Lett. **85**, 1186 (2000).
[10] Y. Liang *et al*., nucl-ex/0410027 (2004).
[11] A. Airapetian *et al.* (HERMES), Phys. Rev. Lett. **90**, 092002 (2003).
[12] W. Melnitchouk, R. Ent, and C. Keppel, Phys. Rep. **406**, 127 (2005).
[13] A. D. Martin, R. G. Roberts, W. J. Stirling, and R. S. Thorne, Eur. Phys. J. C **28**, 455 (2003).
[14] M. Arneodo *et al.* (New Muon Collaboration), Phys. Lett. **B364**, 107 (1995).
[15] J. Gomez *et al*., Phys. Rev. D **49**, 4348 (1994).
[16] I. Niculescu *et al*., Phys. Rev. Lett. **85**, 1182 (2000).
[17] H. Georgi and H. D. Politzer, Phys. Rev. D **14**, 1829 (1976).
[18] S. Dasu *et al*., Phys. Rev. D **49**, 5641 (1994).
[19] C. S. Armstrong, R. Ent, C. E. Keppel, S. Liuti, G. Niculescu, and I. Niculescu, Phys. Rev. D **63**, 094008 (2001).
[20] G. Ricco, M. Anghinolfi, M. Ripani, S. Simula, and M. Taiuti, Phys. Rev. C **57**, 356 (1998).
[21] I. Niculescu, J. Arrington, R. Ent, and C. E. Keppel, hep-ph/0509241 (2005).
[22] J. Arrington, D. Gaskell *et al*., Jefferson lab experiment E03-103.
[23] C. E. Keppel *et al*., Jefferson lab experiment E00-116.
[24] J. Arrington *et al*., Phys. Rev. Lett. **82**, 2056 (1999).
[25] A. Bodek *et al*., Phys. Rev. Lett. **50**, 1431 (1983).
[26] A. C. Benvenuti *et al.* (BCDMS), Phys. Lett. **B189**, 483 (1987).
[27] S. Liuti, private communication.
[28] F. Gross and S. Liuti, Phys. Rev. C **45**, 1374 (1992).
[29] S. A. Kulagin, G. Piller, and W. Weise, Phys. Rev. C **50**, 1154 (1994).
[30] S. Liuti and S. K. Taneja, Phys. Rev. C **72**, 034902 (2005).
[31] E. Marco, E. Oset, and P. Fernandez de Cordoba, Nucl. Phys. **A611**, 484 (1996).
[32] J.-W. Chen and W. Detmold, Phys. Lett. **B625**, 165 (2005).
[33] V. V. Burov, A. V. Molochkov, and G. I. Smirnov, Phys. Lett. **B466**, 1 (1999).
[34] M. E. Christy, C. E. Keppel *et al*., Jefferson lab experiment E02-109.
[35] M. Jones, O. Rondon-Aramayo *et al*., Jefferson lab experiment E01-006.
[36] J. P. Chen, S. Choi, N. Liyanage *et al*., Jefferson lab experiment E01-012.